DOI: 10.1590/2317488920150001004

ARTICLE

Polyphase deformation and metamorphism of the Cuiabá group in the Poconé region (MT), Paraguay Fold and Thrust Belt: kinematic and tectonic implications

Deformação polifásica e metamorfismo do grupo Cuiabá na região de Poconé (MT), Cinturão de dobras e cavalgamentos Paraguai: implicações cinemáticas e tectônicas

Bruno Rodrigo Vasconcelos[1,4,5]*, Amarildo Salina Ruiz[1,2,4,5], João Batista de Matos[1,3,4,5]

ABSTRACT: Several deformation models have been proposed for the Paraguay Belt, which primarily differ in the number of phases of deformation, direction of vergence and tectonic style. Structural features presented in this work indicate that the tectonics was dominated by low dip thrust sheets in an initial phase, followed by two progressive deformation phases. The first phase of deformation is characterized by a slate cleavage and axial plane of isoclinal recumbent folds with a NE axial direction, with a recrystallization of the minerals in the greenschist facies associated with horizontal shear zones with a top-to-the-SE sense of movement. The second stage shows vergence towards the NW, characterized by crenulation cleavage axial plane to F2 open folds over S0 and S1, locally associated with reverse faults. The third phase of deformation is characterized by subvertical faults and fractures with a NW direction showing sinistral movement, which are commonly filled by quartz veins. The collection of tectonic structures and metamorphic paragenesis described indicate that the most intense deformation at the deeper crustal level, greenschistfacies, occurred during F1, which accommodated significant crustal shortening through isoclinal recumbent folds and shear zones with low dip angles and hangwall movement to the SE, in a thin-skinned tectonic regime. The F2 deformation phase was less intense and had a brittle to ductile behavior that accommodated a slight shortening through normal open subvertical folds, and reverse faults developed in shallower crustal level, with vergence towards the Amazonian Craton. The third phase was less pervasive, and the shortening was accommodated by relief subvertical sinistral faults.

KEYWORDS: gondwana agglutination; brasiliano cycle; structural analysis; microtectonic; microstructures.

RESUMO: *Vários modelos deformacionais foram propostos para o Cinturão Paraguai, diferindo principalmente quanto ao número de fases de deformação, sentido da vergência e estilo tectônico. Feições estruturais apresentadas neste trabalho indicam tectônica dominada por escamas de baixo mergulho na fase inicial, seguida por duas fases deformacionais progressivas. A primeira fase de deformação é caracterizada por uma clivagem ardosiana, plano axial de dobras isoclinais recumbentes de direção axial NE, com recristalização de minerais da fácies xisto verde, associada a zonas de cisalhamento horizontais com movimentação de topo para SE. A segunda fase mostra vergência para NW, caracterizada por uma clivagem de crenulação plano axial de dobras abertas de fase F2 afetando S0 e S1, localmente associada a falhas inversas. A terceira fase de deformação é caracterizada por falhas e fraturas subverticais com direção NW mostrando movimentação sinistral, associadas a falhas de alívio, comumente preenchidas por veios de quartzo. O acervo de estruturas tectônicas e paragênese metamórfica descrita indica que a deformação mais intensa ocorreu em nível crustal mais profundo, fácies xisto verde, durante F1, acomodando expressivo encurtamento crustal por meio de dobras isoclinais recumbente e zonas de cisalhamento de baixo ângulo com movimentação de topo para SE, em regime tectônico do tipo pelicular delgado. A fase F2 teve deformação mais sutil e comportou-se ruptil e ductilmente, acomodando discreto encurtamento por meio de dobras normais abertas e falhas inversas subverticais desenvolvidas em nível crustal mais raso, com vergência em direção ao Cráton Amazônico. A terceira fase foi menos intensa e acomodou a deformação na forma de falhas sinistrais subverticais de direção NW.*

PALAVRAS-CHAVE: *amalgamação do gondwana; ciclo brasiliano; análise estrutural; microtectônica; microestrutura.*

[1]Geoscience Postgraduate Program, Institute of Exact and Earth Sciences, Universidade Federal do Mato Grosso – UFMT, Cuiabá (MT), Brazil. *Email: brunovasc@gmail.com*

[2]Department of General Geology, Institute of Exact and Earth Sciences, Universidade Federal do Mato Grosso – UFMT, Cuiabá (MT), Brazil. *Email: asruiz@gmail.com*

[3]Department of Mineral Resources, Institute of Exact and Earth Sciences, Universidade Federal do Mato Grosso – UFMT, Cuiabá (MT), Brazil. *Email: prof.jmatos@gmail.com*

[4]National Institute of Science and Geosciences Technology of the Amazon – GEOCIAM, Universidade Federal do Pará, Belém (PA), Brazil.

[5]Research Group of Crustal Evolution and Tectonics – Guaporé (MT), Brazil.

*Corresponding author.

Manuscrito ID: 30179. **Recebido em:** 10/10/2014. **Aprovado em:** 05/02/2015.

INTRODUCTION

The Poconé region, which has produced gold since the eighteenth century, is in the Internal Zone of the Paraguay Fold and Thrust Belt (Fig. 1). The region was developed between the Amazon and Paranapanema Cratons during the amalgamation of the Gondwana Supercontinent in the Neoproterozoic. Several studies published since the work of Evans (1894) have characterized this belt according to different geological aspects; however, important questions on the evolution of this tectonic province remain under discussion. Several authors have discussed the deformational evolution of the belt and have proposed different deformational phases in different regions of the belt that are not clearly correlated. For example, in the southern region of the belt near Bonito and Aquidauana in the state of Mato Grosso do Sul, Almeida, (1965b, 1984), Nogueira and Oliveira (1978), Corrêa *et al.* (1979) and Campanha *et al.* (2011) assigned three phases of coaxial deformation with vergence towards the Rio Apa Block, which is a southern extension of the Amazon Craton. In the central region of the belt near Cuiabá and Província Serrana of Mato Grosso, Luz *et al.* (1980) and Souza (1981) assigned three phases of coaxial deformation, Pires *et al.* (1986) assigned two phases of coaxial deformation and a transversal phase, and Silva *et al.* (2002) observed three phases of coaxial deformation and a transversal phase. In the extreme east of the belt, in the region of Bom Jardim of Goiás in the state of Goiás, Seer (1985) and Seer and Nilson (1985) assigned three phases of coaxial deformation, as well as one orthogonal phase, and also observed that this part of the belt shows SE vergence in contrast to the Amazon Craton, which was also observed by Del'Rey Silva (1990). That author explained the inversion by proposing a thrust and back thrust model, assuming the second deformation phase was generated during back folding following the first deformation phase. The metamorphic history and age of the metamorphic peak reached by the belt, which marked the culmination of the Brasiliano orogeny in the region, are also currently under discussion.

This multiscale structural analysis study aimed to descriptively and kinematically characterize the three phases of deformation observed in the rocks of the Poconé region, relating them to their metamorphic and deformation conditions, which is a different approach to the work that has already been performed in the Poconé region, whose goal was characterizing the mineralization.

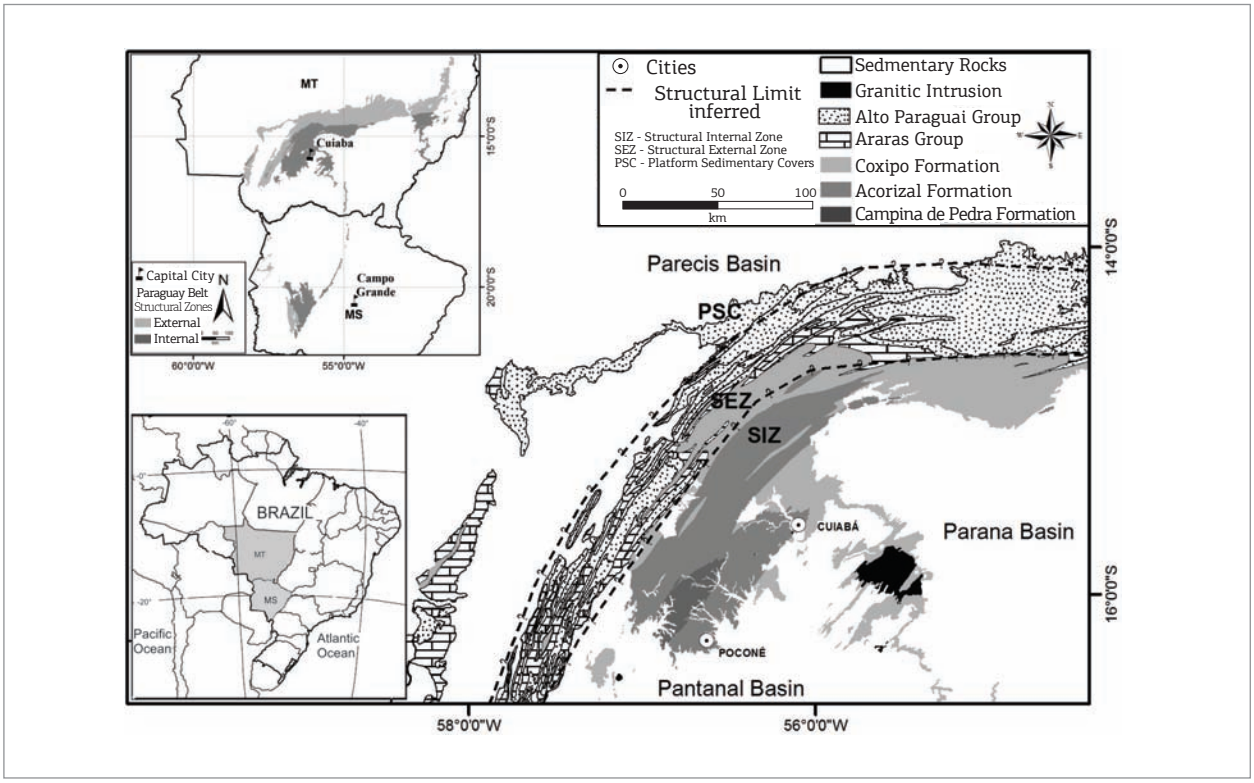

Figure 1. Map of the Paraguay Belt (detail at top left) and the regional geological setting of the study area in the Poconé region based on the stratigraphic study of Tokashiki and Saes (2008) (Geological map extracted from Lacerda Filho *et al.* 2004).

METHODS

The data presented in this paper were obtained from open pits in the municipality of Poconé and the Cangas district (Fig. 2), which are located along the Cangas-Poconé Alignment, which trends N40E and hosts the primary mineral occurrences of the Gold Province of Baixada Cuiabana (Paes de Barros *et al.* 1998). Because of the large number of pits that occur in this region, the pits selected were the ones which had a high occurrence of structures that showed the superposition of the identified deformational phases. The rock types that make up the Cangas Facies of the Acorizal Formation in these pits are mainly phyllites, metasandstones, metaconglomerates and diamictic levels. All have a strong magnetic signature, as described by Tokashiki and Saes (2008), who further describe them in terms of their rheological characteristics and deformation, especially their responses to the stresses and metamorphic conditions to which they were submitted during the deformational processes. The morphological descriptions of structural features, as the concepts of deformation phases and progressive deformation, were based on Fossen (2012). The microstructural description was based on concepts proposed by Passchier and Trouw (2005) and Vernon (2004); the latter was also used for the abbreviation of the minerals identified microscopically.

GEOLOGICAL SETTING

The Paraguay Fold and Thrust Belt is located along the southeastern Margin of the Amazon craton (Almeida 1965b), with folded metasedimentary rocks that show a decrease in deformation and metamorphism intensity towards the Amazon craton. Almeida (1984) subdivided the belt structurally into three zones: the Metamorphic Brasilides, Non-Metamorphic Brasilides and Brasiliano Cover, which were subsequently called the Metamorphic, Structural Internal Zone with granitic intrusions (SIZ); Non-Metamorphic, Structural External Zone (SEZ); and Platform Sedimentary Cover (PSC) by Alvarenga and Trompette (1993) (Fig. 1). The SEZ is characterized by isoclinal folding, low-grade metamorphism and post-orogenic granite intrusions. It is characterized by open folding with reverse faulting and associated anquizonal or non-existent metamorphism. The transition between the two zones occurs by reverse faulting (Alvarenga & Trompette 1993). The PSC is characterized by gentle undulations, nonexistent metamorphism and non-penetrative brittle tectonics. Alvarenga (1988, 1990) described the Paraguay Belt as a polyphase folding belt that was affected by the Brazilian Cycle. Regarding the stratigraphy, several deformation models have been proposed (Fig. 2A), including three coaxial deformation phases (Nogueira & Oliveira 1978; Corrêa *et al.* 1979; Almeida 1965b, 1984; Luz *et al.* 1980; Souza 1981), two coaxial deformation phases and one transversal phase (Pires *et al.* 1986), and three coaxial deformation phases and one orthogonal phase (Seer 1985; Seer & Nilson 1985). Silva (1999) and Silva *et al.* (2002) proposed three coaxial deformation phases (Fig. 2B) and one orthogonal phase, and also indicated the presence of a foliation pre-Dn event.

In addition to the number of phases that affected the SIZ of the belt, vergence is also currently being discussed. Some authors have considered a SE vergence for the initial

A

Authors	Deformation Stages				
	1	2	3	4	5
Luz *et al.* (1980)	D1	D2		D3	
D'el-Rey Silva (1990)	D1	D2		D3	D4
Alverenga (1990) Alvarenga & Tompette (1993)		D1	D2	D3	D4
Silva (1999); Silva *et al.* (2002)	Dn-1(?)	Dn	Dn+1	Dn+2	Dn+3
Barbosa (2004?)		Dn*		Dn+1**	Dn+2***

The asterisk differenctiate the vergence observed, therefore (*) show the vergence to SE and NW making range, (**) show the vergence to NW, and (***) show the vergence to SW.

B

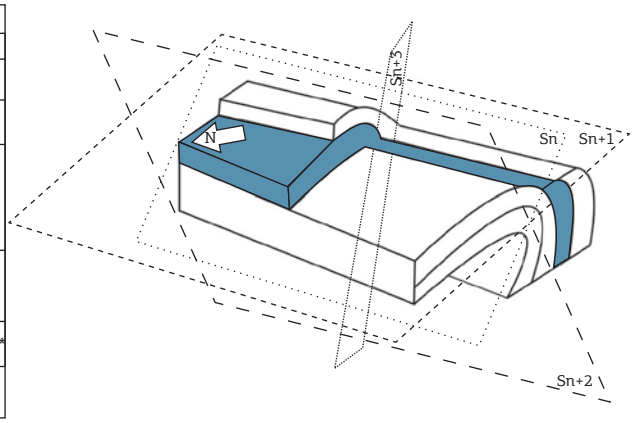

Figure 2. (A) A comparison between the main deformation models already proposed for the structural internal zone of the belt (modified from Barbosa 2008). (B) It presents the schematic model of the deformation phases proposed by Silva *et al.* (2002) (modified from Silva *et al.* 2002).

stage (Silva *et al.* 2002), while others have interpreted a NW vergence for the initial stage (D'el-Rey Silva 1990). The deformation age is also a controversial issue because a single Rb-Sr age from phyllite published by Barros *et al.* (1982) provided an age of 481 ± 19 Ma, which was interpreted as the final stage of the orogenic evolution. However, De Min *et al.* (2013) dated undeformed ultramafic rocks intruded into rocks of the Cuiabá Group and Puga Formation using the Ar-Ar, Sm-Nd and Rb-Sr methods, and obtained approximate ages of 600 Ma, which indicate that the onset of deformation and active metamorphism of rocks in the Cuiabá Group are older than 600 Ma; the author also suggested that these events must have occurred during the Cryogenian–Ediacaran transition. What most authors agree on is that the belt evolution occurred during the Brasiliano deformation was continuous, superimposed deformation was present and the greatest intensity occurred in the first two stages. There is no evidence of oceanic crust or magmatic arc related to subduction of oceanic lithosphere in the region of Cuiabá, but at the eastern extreme of the belt there are volcano-sedimentary sequences with lithological and geochemical characteristics that suggest an evolution similar to that of current island arcs (Alvarenga 1990). Post-tectonic granitic intrusions approximately aged 500 Ma (Godoy *et al.* 2010) sealed the orogenic event along with the orogeny collapse; these intrusions were divided by Manzano *et al.*(2008) e Godoy *et al.* (2010) into two groups: one further north, with characteristics of anorogenic Magmatism (São Vicente, Lajinha and Araguaiana granites), and another further south, with magmatic arc characteristics (Taboco, Rio Negro, Coxim and Sonora granites). The belt rocks can be divided into three lithologic associations: a lower turbidite-glaciogenic, an intermediate carbonated, and an upper detrital (Alvarenga 1988; Alvarenga & Saes 1992; Alvarenga & Trompette 1993). Several columns of these associations have been proposed, and the main ones were compared with the most recent stratigraphic stacking proposed by Tokashiki and Saes (2008) (Fig. 3). They represented the Cuiabá Group as the lower and intermediate units identified by Alvarenga and Trompette (1993) and divided it from bottom to top into the Campina of Pedras, Acorizal and Coxipó formations; the upper unit is represented by the Araras and Alto Paraguay groups. In the study area, (Fig. 3) lithologies from the middle part of the Acorizal formation of Tokashiki and Saes (2008) are exposed, which are called the Cangas Facies. These rocks are predominantly metarhythmites with dropstones deposited under a strong glacial influence. The facies

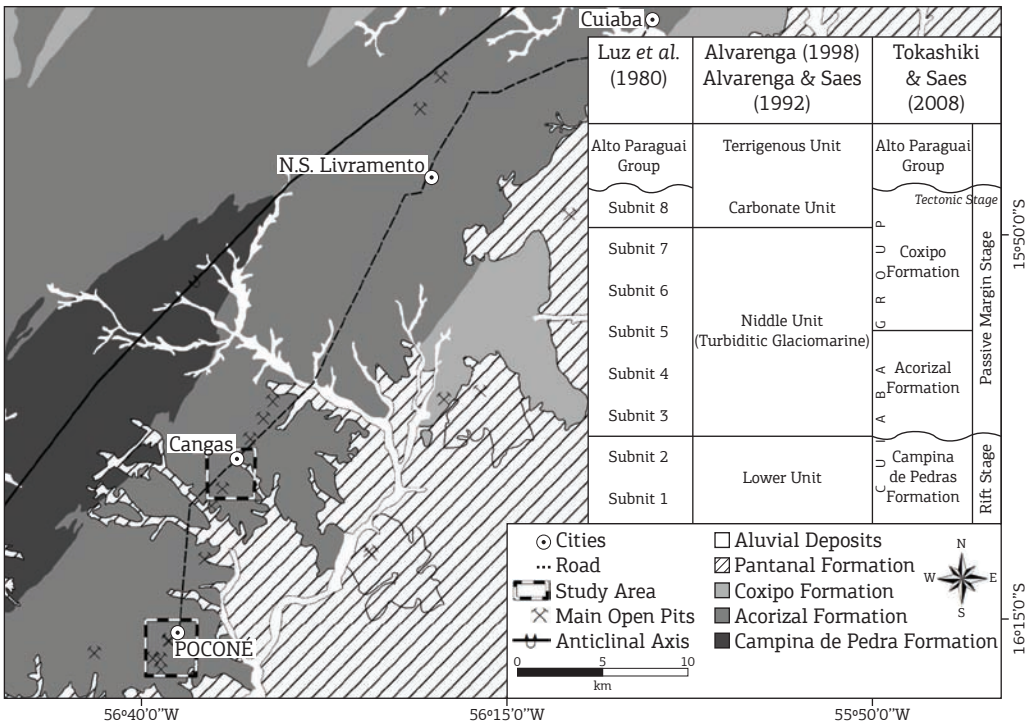

Figure 3. Simplified geological map of the studied areas and a comparison between the main stratigraphic column proposals and the recent stratigraphic review by Tokashiki and Saes (2008).

occurs in association with metaconglomerates, metasandstones, phyllites and subordinate horizons of massive metadiamictites. These are interpreted as having been deposited during a long deglaciation period with an eustatic sea level rise and the release of coarse clasts from icebergs.

STRUCTURAL ANALYSIS

Primary structures - S0

Layering (S0) is the most outstanding feature observed in the walls of the pits, which are defined by the variation of colors, composition, grain and layer thicknesses that compose the predominantly rhythmic units that occur in the region. The S0 poles (Fig. 4A) suggest a girdle that indicates open folding with an intermediate subhorizontal axis trending N020E and two maximum concentrations of poles within the girdle matching the flanks of the folds; maximum concentrations at approximately N021E/22SE and N033E/31NW due to refolding occurred in the second deformation stage (F2). The stratigraphic top is difficult to define because the observed stratification is mainly plane-parallel and occurs in large tight isoclinal recumbent folds (D1) that are attributed to the first deformation stage (F1), with the axial plane usually subparallel to the layering.

First deformation phase - F1

The first deformation phase (F1) active in the region was the most intense and responsible for the main accommodation of shortening in the region. This phase is marked by intense slaty cleavage (S1) (Fig. 4D), axial plane of asymmetrical folds (D1), recumbent, non-cylindrical, with apical thickening, isoclinal to closed, with axes and intersection lineations (Lb1) between the S0 and S1 plans with an average attitude N026E/07 parallel to the direction of S0 and S1 (Fig.4A). This stage accommodated the main shortening recorded in the rocks in the study area and marked the most intense active deformation and metamorphism during the development of this stage, which reached the greenschist facies biotite zone as described latter. The parallelism of S0 to S1 makes it difficult to visualize the latter, which is only differentiated from S0 in hinge areas of the D1 folds. The preferred attitude of S1 is subparallel to S0, trending N020E/40SE, sometimes dipping NW and trending N014E/26NW, and establishing a girdle due to refolding caused by F2. Stretching lineations (Lx1) contained in S1 show a subhorizontal attitude towards the dip of this foliation, N060E/14, and in places where S1 dips NW to N077W/09 (Fig. 4A), with kinematic indicators such as folds, tension gashes and clasts with pressure shadows that indicate that the mass displacement was predominantly towards the SE during this stage (Fig. 4E). This movement was accommodated by subhorizontal faults parallel to S1, which worked as thresholds for the displacement (Fig. 4F), indicating that fault nucleation occurred in the post-F1 stages when most of the D1 folds were already generated and S1 was developed, once faults nucleated along S1 plans near the lithological contrasts. A large amount of quartz veins occur parallel to S1 and are folded into the same style and attitude as D1, which indicates greater metamorphic fluid input during that stage of development.

Second deformation phase – F2

This phase was also quite intense in rocks of the region and was possibly caused by the continuous shortening that began in F1 during progressive deformation. The phase is defined by a penetrative foliation (S2) filled with products from pressure dissolution (Fig. 5A) and crystallization of metamorphic minerals oriented in relation to the S2 plane. S2 defines the main plane of rock fracturing and has an average attitude of N25E/80SE, parallel to S1 (Fig. 4B), but because of its high angle, dips to the NW are commonly found. This stage is characterized by more intense structures, which are numerous and well developed near the sub-vertical fault ramps that were generated in F1, where the occurrence of reverse faulting and the development of quartz veins that are parallel to the S2 planes is common. S0 and S1 crenulation, the smaller spacing between the septum and an increase in the amount and intensity of filling material by pressure dissolution and metamorphic crystallization (Fig. 5A), are also common near these faults. The septa become more spaced and present a less developed crenulation as the distance increases from the fault zones, the metric folds give rise to decametric folds whose axial plane is subparallel to S2 (Fig. 5B) and dips SE, and the foliation is much less developed. The D2 folds, because the scale of the crenulations to the decametric folds are normal, open to soft, with a sub-horizontal axis in a NE direction and sub-vertical axial plane (Fig. 4B), and the intersection lineation between S1 and S2 (LB2) show an attitude that is parallel to the D2 axes as well as to the lineation Lb1 and to the axes of the D1 folds, which established the coaxiality between stages F1 and F2. (Fig. 4A). Especially in the crenulations, note that the longer flank usually dips SE, which indicates a vergence towards the NW (Fig. 5A and 5B); the same pattern is shown in the average attitude of S2 (Fig. 4B), where a single concentration of poles reinforces that these planes are not folded. This phase accommodated less intense shortening than during F1, accommodating ductile and brittle behavior mainly through the D2 folds and sub-vertical reverse faulting associated with S2, showing metric tailings and associated drag folds.

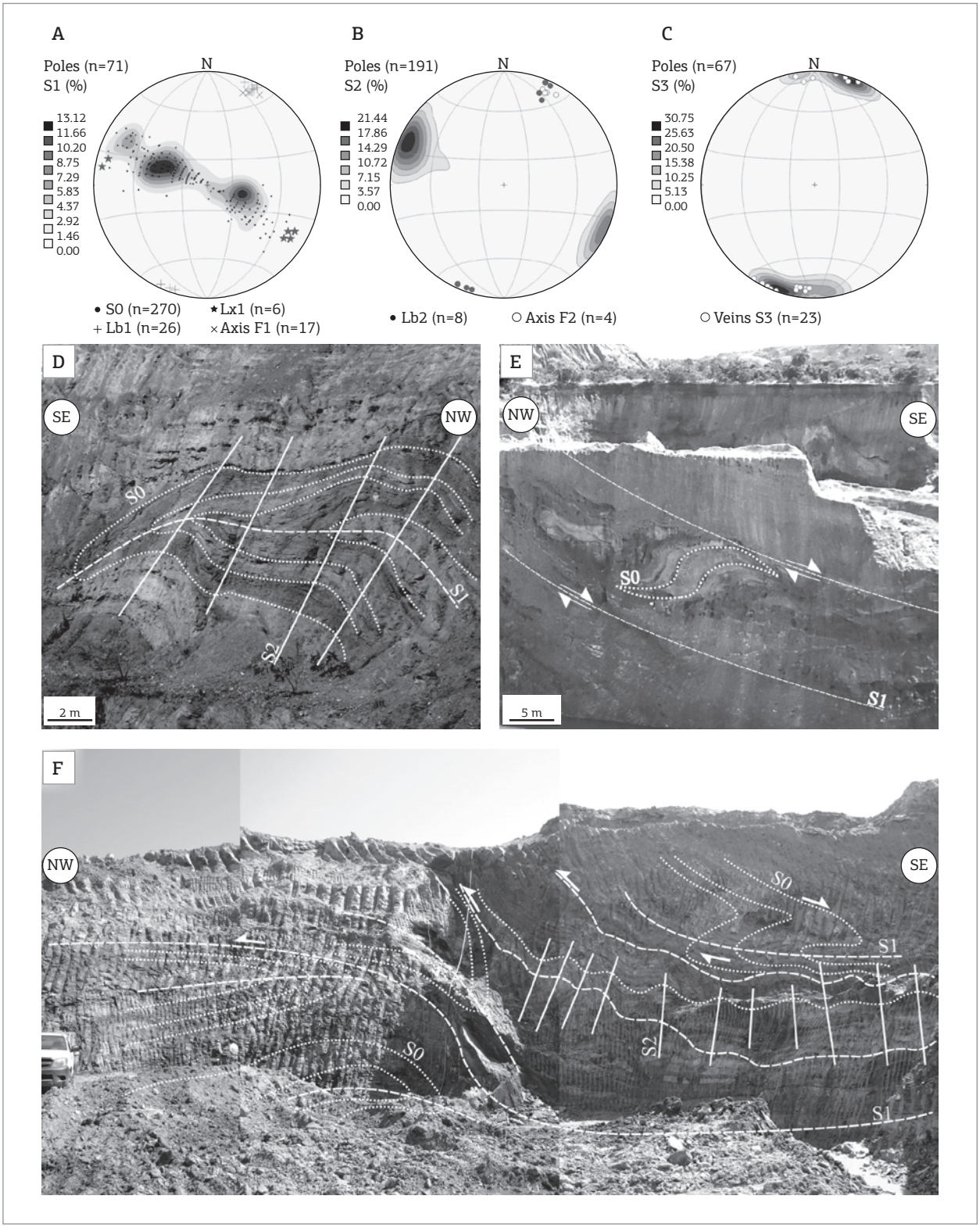

Figure 4. (A) Polar Isofrequency stereogram of S1, compared to the poles of S0, intersection lineations between S0 and S1 (Lb1), D1 fold axes (D1 axis) and stretching lineations (LX1). (B) Polar Isofrequency stereogram of S2, compared to intersection lineations of S1 and S2 (LB2) and the D2 fold axes (D2 axis). (C) Polar Isofrequency stereogram of S3, compared to the poles of the S3 veins. Stereograms using lower hemisphere. (D) Folds of the layers showing planes and folds generated in the two early coaxial phases F1 and F2. (E) Folded layers showing top motion towards the SE associated with sub-horizontal faults in the S1 plane. (F) Sub-horizontal faulting associated with F1, with folded layers (D1) indicating top motion towards the SE.

Third deformation phase – F3

This phase predominantly accommodated the brittle effort and is characterized by sub-vertical fractures and faults commonly filled by quartz veins. With an average attitude of N70W/83NE, it is usual to find dips to the SW (Fig. 4C). The thickness, spacing, presence and filling intensity along plans vary according to the rheological behavior and composition of the rocks. By using planar markers, a sinistral kinematic is identified along these plans when observed in plan view (Fig. 5C) and normal when observed in profile view (Fig. 5D). The apparent horizontal component always shows centimetric reject because the vertical reject shows metric tailings. A single friction striation contained along a fault plane indicates that a normal motion (down dip) occurred later and apart from a sinistral motion (strike-slip), but this statement still requires more field data. The quartz veins associated with these planes are fractured and deformed in relation to the planes that are parallel to the S1 and S0 planes, which might indicate that part of the veins in the WNW direction is related to the post-F1 and F2 phases.

METAMORPHISM AND MICROSTRUCTURES

Under the microscope, the first deformation phase F1 is identified as being responsible for the main metamorphic event active in the region (M1), whose main mineral assemblage consists of biotite (Bt), chlorite (Chl) and muscovite (Ms) crystallized in relation to the S1 plan (Fig. 6A). It is defined by

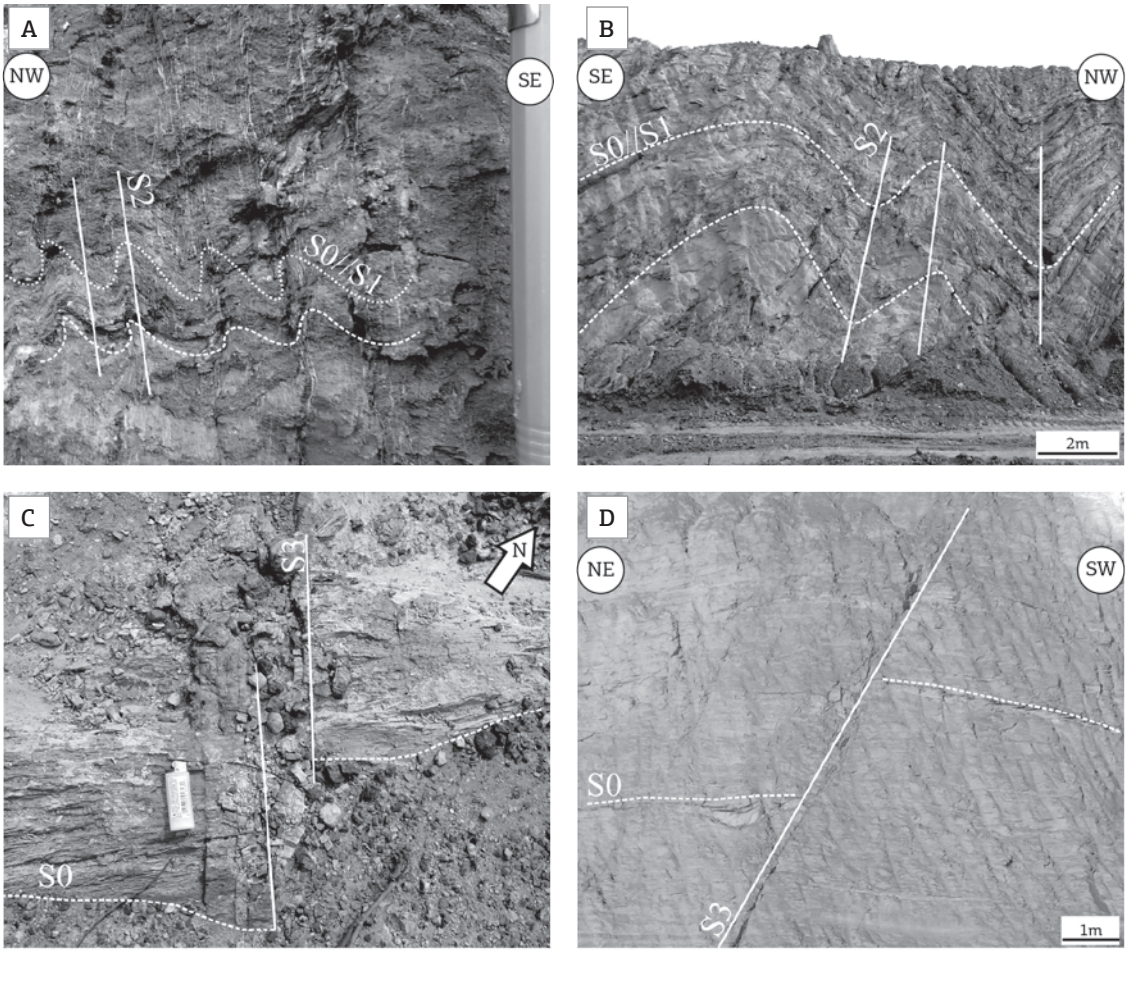

Figure 5. (A) S2 foliation defined by septa filled by a pressure dissolution material and causing the crenulation of S0 and S1 with folds (D2) showing a longer flank dipping SE. (B) Metric normal open folds (D2), showing a longer flank dipping SE and the S2 foliation axial plane. (C) Sinistral faulting with centimetric reject associated with S3, plan view. (D) Normal faults with metric reject associated with S3, profile view perpendicular to the plane.

a continuous anastomosing foliation and slaty cleavage, and is fine grained with a granolepidoblastic texture. The mechanisms of the development of this foliation were the crystallization of oriented metamorphic minerals (mica), dynamic recrystallization, mainly quartz (Qtz) and recovery by the intracrystalline deformation of blasts and clasts. The metamorphic crystals are developed as subhedral crystals up to 0.5 mm in phyllites and as euhedral thin needles smaller than 0.1 mm in metasandstones. The larger micas commonly are biotite, locally chloritized, and sometimes presenting wavy extinction, lamellae deformation and individualized subgrains along planes subparallel to S1. The needles are predominantly muscovite and are always developed in contacts between quartz grains.

Dynamic recrystallization occurs mainly in quartz grains (Fig. 6B), through bulging recrystallization (Passchier & Trouw 2005) around grain boundaries, and subgrain rotation (Vernon 2004) defined by the rotation of individual quartz grains that are able to modify its extinction position. Intracrystalline deformation (Passchier & Trouw 2005) occurs mainly in quartz, but is also observed in some larger micas. It is identified by wavy extinction, lamella and deformation bands, and the latter commonly appear as the barrier for ancient quartz grains within the subgrains and are locally replaced by metamorphic minerals (mica) that give the elongated shape for the new boundaries of quartz crystals. The filling of plans by opaque residues due to pressure dissolution (dissolution-precipitation – Passchier & Trouw 2005) are common around the contacts between quartz and clay lenses. The degree of deformation and metamorphic process is more intense in samples located near faults that were

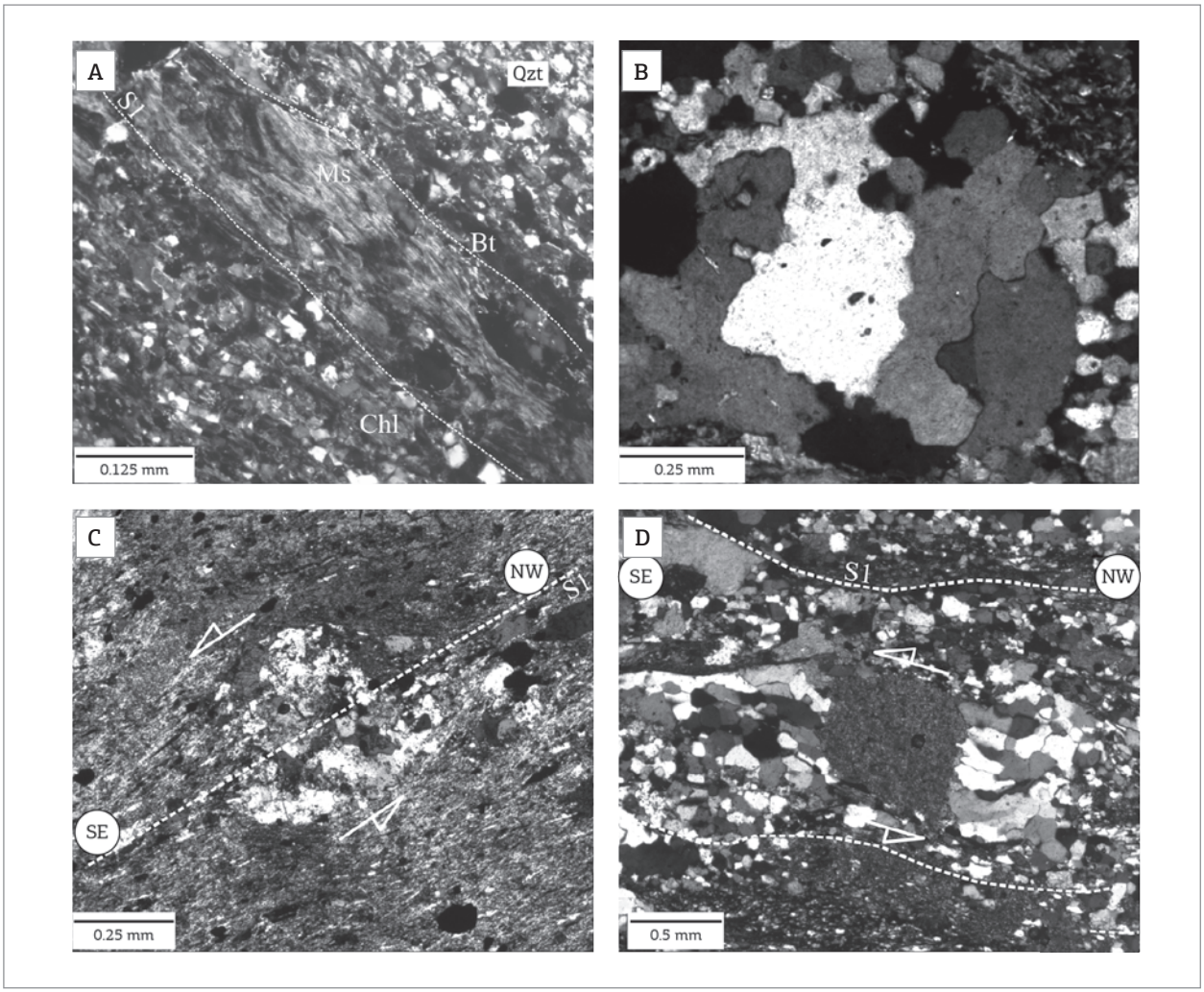

Figure 6. (A) Metamorphic assemblage developed by F1; note the difference between the quartz and micaceous levels that define the S1 plane. (B) Details of the recovery and recrystallization mechanisms acting on the quartz grains. (C) Sigma-type strain shadow showing sinistral kinematics with top motion towards the SE. (D) Sigma-type antitaxial strain fringe showing sinistral kinematics with top motion towards the SE.

nucleated during S1, mainly in phyllites, while less intense far from faults and/or in metasandstones. The asymmetry of kinematic indicators, such as deformation shadows (Fig. 6C) and fringes (Fig. 6D), occurs mainly in quartz clasts within conglomerate levels and some metasandstone levels with more intense dynamic recrystallization. These indicate a dominant motion to the SE in agreement with the macroscopic observations. The age for M1 is still uncertain and will require a specific dating method.

The second deformation phase, F2, is recorded in rocks as a spaced foliation, and the type crenulation cleavage is smooth and parallel (Fig. 7A). Microliths are defined by S1 plans, oriented and gently folded, and with an axial plane that defines the S2 septum. The folding of microliths is accommodated by micas with a brittle behavior through fractures and faults that rotate crystals which define the fold morphology and through recovery processes such as wavy extinction in quartz, deformation lamella and bands, and dynamic recrystallization through subgrain rotation. The septa are mainly defined by mica produced during S1 that are almost orthogonally reoriented, which causes a change in the extinction position, that in turn causes microliths and septa to become extinct in different directions, which is easily identifiable with crossed polarizers. The crystallization of muscovite (Fig. 7B) and dynamic recrystallization by subgrain rotation restricted to grain boundaries occurs in quartz, where the intensity of F2 was more intense. Where F2 was less intense there is often no septum, making the open folding the only feature recorded in relation to F2; in addition to the occurrence of chloritized biotite, the local precipitation of residues caused by pressure dissolution is also a feature of the

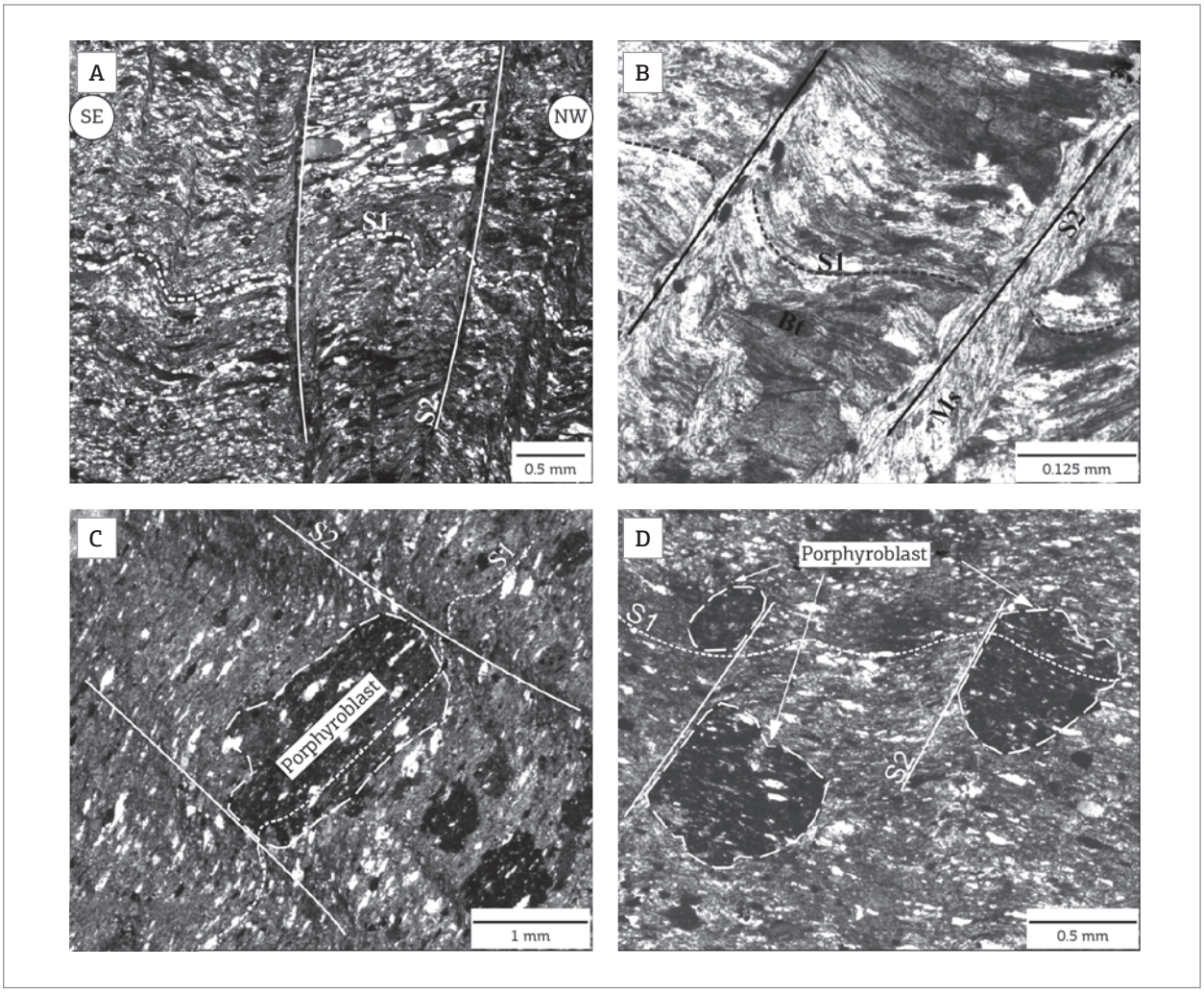

Figure 7. (A) Crenulation cleavage as a product of F2; note the longer flank dipping SE. Microliths defined by S1 and septa defined by S2. (B) Crystallization of muscovite along S2 planes. (C) Carbonate porphyroblast superimposed on the S1 foliation. (D) Carbonate porphyroblast growth limited by S2 planes.

septa in those sites. The asymmetry of the folded microliths follows the same pattern of macroscopic features in which the long flank dips SE, indicating a NW vergence for this phase (Fig. 7A).

The third, orthogonal deformation phase, F3, generated no microscopically observable planes. In thin sections an intense fracturing is observed, which operated in both micaceous minerals and quartz, but does not define a plane. The recovery and recrystallization features appear to be products of the earlier phases.

The growth of carbonate porphyroblasts and opaque crystals of magnetite and pyrite shows a clear temporal relationship that indicates post-F1 growth because they are grown on the S1 foliation (Fig. 7C and 7D) and do not present deformation shadows or fringes. These are likely post-S2 because the crenulation is perfectly printed within the carbonate porphyroblasts, and some of them had their growth limited by the septum of S2 (Fig. 7D). No relationship was found between the growth of porphyroblasts and the development of F3.

DISCUSSION AND CONCLUSIONS

The presence of biotite, muscovite, chlorite and quartz in the S1 foliation indicates that during the first deformation phase (F1) the metamorphic conditions acting on the rocks of the region reached the greenschist facies, biotite zone. This is consistent with the microstructural features observed in F1, because, according to Passchier and Trouw (2005) and Vernon (2004), the predominance of subgrain rotation recrystallization, widely performed by recovery mechanisms and crystals flattening, are phenomena that occur under these conditions. The occurrence of these conditions is corroborated by the dominant ductile deformation that accommodated the active shortening during F1. The morphology of the structures observed in this phase indicates that the beginning of the active shortening in F1 acted with a southeast vergence, towards interior the belt, probably in response to Paranapanema craton collision. This shortening was responsible for the folding by simple shear that produced the D1 folds, accommodating the maximum shortening and reaching the peak metamorphic, greenschist facies, biotite zone. In addition to the intense folding, shortening was also accommodated by subhorizontal faults that formed along the S1 foliation planes (Fig. 8A), mainly where the faults were parallel to lithological/rheological discontinuities. These faults were described by D'el-Rey Silva (1990) in a tectonic model that involved flaking by NW-verging thrust faults during the D1 stage, followed by backthrusting towards the SE during the D2 and D3 progressive stages. However, the D'el-Rey Silva model was later discarded due to the absence of low-angle penetrative structures in the northern portion of the structural internal zone and the fan-shaped geometry of the main foliation.

The veins associated with these faults are correlated to the linear elongated subhorizontal veins trending NE described by Costa *et al.* (2008) and Paes de Barros *et al.* (1998), which are associated with average contents of approximately 1 g/tonne. The authors also associated this phase with bidirectional subvertical tabular veins called *filões* and *travessões* in the NW and NE directions, respectively. The former have average levels of 5 g/tonne. The latter, have NE orientation of the main mineralized lineaments, called Salinas-Praia Grande and Cangas-Poconé, which separates the stratigraphic units and show hydrothermal alteration halos. As described above, the kinematic indicators of the F1 phase show a top-to-the-SE sense of movement at multiple scales, and, because the faults are always associated with S1 foliation, their formation is attributed to the final stages of F1; that is, the faults would be post-F1 and pre-F2 once the fault planes were affected by the D2 folds. The dominant ductile deformation behavior of this phase indicates that the rocks were deeper than 12 km. For the second deformation phase (F2), the brittle behavior of biotite crystals that accommodated shortening through kinks is typical for temperatures below 250°C, according to Stesky *et al.* (1974) and Stesky (1978). This is corroborated by the intense fracturing, subgrain rotation recrystallization and recovery processes of the quartz crystals, in addition to the intense precipitation of residual material caused by pressure dissolution along the S2 planes. Such features, according to Dunlap *et al.* (1997), Van Darlen *et al.* (1999), Stipp *et al.* (2002) and Nishikawa and Takeshida (1999), are characteristic temperature phenomena below 300°C, which is consistent with white mica crystallization (Ms) along the S2 planes under low grade metamorphism and the dominant reorientation of the micas formed during F1. These characteristics are consistent with the brittle-ductile deformation settings observed in the F2 structures. According to Pluijm and Marshak (2004), the interface between ductile and brittle behavior occurs at depths of approximately 10 km, which indicates that these rocks were uplifted to shallower crustal levels during F1, modifying the PT conditions. These changes caused the accommodation of active shortening during F2 to be predominantly brittle in competent rock types and to be brittle-ductile in less competent rock types through folding by passive pure shear, which resulted in the D2-folds and the subvertical reverse faults produced along the S2 planes of foliation (Fig. 8B). The change of vergence during this phase indicates that at that time the Amazon craton was the main continent for the belt, being nearest due to the intense active shortening during F1.

The third deformation stage (F3) only shows brittle deformation on the quartz and mica grains, and the precipitation of residual material along the fracture planes resulted from pressure dissolution; according to Dunlap *et al.* (1997), Van Darlen *et al.* (1999), and Stipp *et al.* (2002), these features are also characteristic of phenomena below 300°C. These conditions, along with the macroscopic features such as faults and fractures, indicate that the last phase, F3, acted under pure brittle conditions at even smaller depths than for F2. The sinistral strike-slip kinematics associated with the S3 faults (Fig. 8C) is interpreted as a result of the shortening that began during F1 and was also active in F2 by progressive deformation, producing release faults that were orthogonal to the shortening direction during the latter stage. However, thin sections of veins hosted in the S3 faults show deformation bands and deformation lamellae in planes parallel to S1 and fractures parallel to S2, which indicate the performance of the F1 and F2 stages. This indicates that some of these veins might be related to the early stages, F1 and F2, and are thus correlated to the NW veins described by Costa *et al.* (1998) and Paes de Barros *et al.* (1998), which differ from the veins produced in F3 due to the recognition of prior deformation. The S2 and S3 planes also show signs of reactivation in latter stages (drift) or subsequent to the Brasiliano orogeny and developed normal kinematics, which probably reflected the opening of Phanerozoic and Mesozoic basins on the South American platform.

The deformational and metamorphic characteristics indicate that the main approximation between the Amazon and Paranapanema continents occurred during the first deformation stage. The latter craton served as the primary deformation shield, which is recorded in the tectonic transport towards the SE. This stage possibly records the beginning of the amalgamation process of the Gondwana supercontinent in the region.

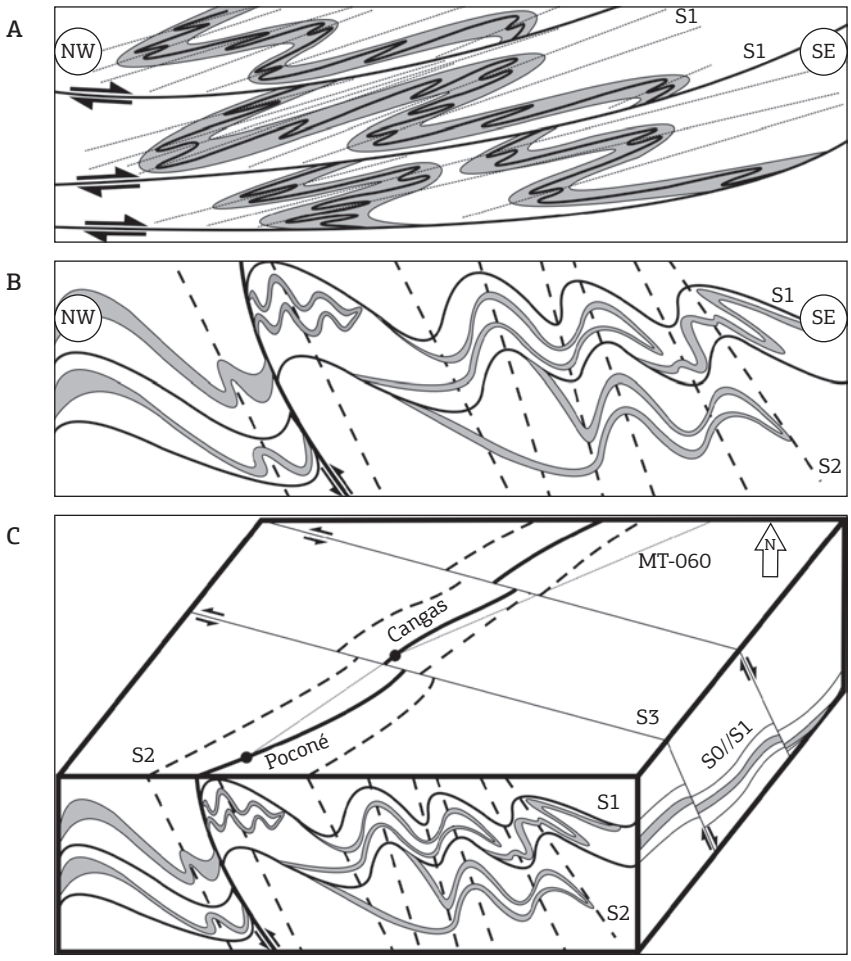

Figure 8. Model for the tectonic evolution of the Cuiabá Group in the Poconé region (MT), highlighting the overlap of the deformation phases. (A) Features related to the first phase. (B) Features related to the second phase. (C) 3D sketch showing the proposed regional structure as a result of the three proposed deformation phases.

Subsequent deformation stages occurred progressively and recorded the final stages of the progress of the construction of the Paraguay Orogen during the amalgamation of West Gondwana, which accommodated less intense shortening and set the structural and metamorphic framework of the belt. However, because the approximation of the Amazonian Craton occurred during the initial stage, this craton became the main shield for the final deformation, recording a tectonic transport towards the NW. The metamorphic conditions show that the rocks in the area were being uplifted to shallower depths as the deformation occurred.

ACKNOWLEDGMENTS

The authors thank the following institutions for their technical and financial support: the Geoscience Postgraduate Program (PPGEC), National Institute of Science and Geosciences Technology of the Amazon (GEOCIAM), Universidade Federal do Mato Grosso (UFMT) and the Mineral Development Cooperative of Poconé (COOPERPOCONÉ). The authors also thank the reviewers for their valuable contribution to this work. Special thanks to Kamila G. Fernandes for the English version of the paper.

REFERENCES

Almeida, F.F.M. 1965a. *Geologia da Serra da Bodoquena (Mato Grosso)*. Rio de Janeiro, DNPM/DGM, 96 p. (Boletim 219).

Almeida F.F.M. 1965b. Geossinclíneo Paraguai. *In*: Semana de Debates Geológicos, 1, Porto Alegre, Centro Acadêmico dos Estudantes de Geologia, Universidade Federal do Rio Grande do Sul, *Atas*, p.87-101.

Almeida F.F.M. 1984. Província Tocantins - setor sudoeste. *In*: Almeida, F.F.M. & Hasui, Y. eds. O *Pré-Cambriano do Brasil*. São Paulo, Ed. Blücher, p. 265-281.

Alvarenga C.J.S. 1988. Turbiditos e a glaciação do final do Proterozóico Superior no Cinturão Paraguai, Mato Grosso. *Revista Brasileira de Geociências*, **18**:323-327.

Alvarenga C.J.S. 1990. *Phénomènes Sédimentaires, Structuraux et Circulation de Fluides Développés à La Transition Chaîne-Craton: Exemple de la Chaine Paraguai d 'age proterozoique supérieur, Mato Grosso, Brésil*. These Doct. Sei, Université d'Aix-Marseille III, Marseille, 177 p.

Alvarenga C.J.S. & Saes G.S. 1992. Estratigrafia e Sedimentologia do Proterozóico Médio e Superior da região sudeste do Cráton Amazônico. *Revista Brasileira de Geociências*, **22**(4):493-499.

Alvarenga C.J.S. & Trompette R. 1993. Brasiliano tectonic of the Paraguai Belt: the structural development of the Cuiaba region. *Revista Brasileira de Geociências*, **23**:18-30.

Barbosa E.S. 2008. *Gênese e Controle Estrutural das Mineralizações Auríferas do Grupo Cuiabá, na Província Cuiabá-Poconé, Centro Sul do Estado de Mato Grosso*. Tese de Doutorado, Universidade do Estado do Rio deJaneiro, Rio de Janeiro, 155p.

Barros A.M., Adalberto R.H., Cardoso O.R.F.A., Freire F.A., Souza J.J., Rivete M., Luz D.S., Palmeira R.C.B., Tassinari C.C.G. 1982. *Folha SD. 21 Cuiabá, Projeto RADAMBRASIL. Levantamento de Recursos Naturais*. Rio de Janeiro, Ministério das Minas e Energia,v. 26, p. 25-192.

Campanha G.A.C., Boggiani P.C., Filho W.S., Sá F.R., Zuquim M.P.S., Placentini T. 2011. A Faixa de Dobramentos Paraguai na Serra da Bodoquena e Depressão do Rio Miranda, Mato Grosso do Sul. São Paulo, *Geologia USP, Série Científica*, **11**(3):79-96.

Corrêa J.A., Correia Filho F.C.L., Scslewski G., Neto C., Cavallon L.A, Cerqueira N.L.S., Nogueira V.L. 1979. *Geologia das Regiões Centro e Oeste de Mato Grosso do Sul*. Brasília, DNPM. 111 p. (Geologia Básica 3).

Costa J.L.G., Ruiz A.S., Weber F., Paes de Barros A.J. 1998. Controle Estrutural do Depósito Aurífero da Fazenda Salinas, Poconé-MT. *In*: XL Congresso Brasileiro de Geologia, Belo Horizonte, *Anais*, SBG-MG.

D'el-Rey Silva L.J.H. 1990. Ouro no Grupo Cuiabá, Mato Grosso: controles estruturais e implicações Tectônicas. *In*: XXXVI Congresso Brasileiro de Geologia, Natal, *Anais SBG*, **6**:2520-2534.

De Min A., Hendriks B., Slejko F., Comin-Chiaramonti P., Girardi V., Ruberti E., Gomes C.B., Neder R.D., Pinho F.C. 2013. Age of Ultramafic High-K rocks from Planalto da Serra (Mato Grosso, Brazil). *Journal of South American Earth Sciences*, **41**:57-64.

Dunlap W.J., Hirth G., Teyssier C. 1997. Thermomechanical Evolution of a Ductile Duplex. *Tectonics*, **16**:983-1000.

Evans J.W. 1894. The geology of Mato Grosso. *Quarterly Journal, Geological Society of London*, **50**(2):85-104.

Fossen H. 2012. *Geologia Estrutural*. Trad. de Fabio R.D. de Andrade. São Paulo, Oficina de Texto, 584 p.

Godoy A.M., Pinho F.E.C., Manzano J.C., Araujo L.M.B., Silva J.A., Figueiredo M. 2010. Estudos Isotópicos das Rochas Granitóides Neoproterozóicas da Faixa de Dobramento Paraguai. *Revista Brasileira de Geociências*, **40**(3):380-391.

Lacerda Filho J.V., Abreu Filho W., Valente C.R., Oliveira C.C., Albuquerque M.C. 2004. *Geologia e Recursos Minerais do Estado de Mato Grosso: texto explicativo dos Mapas geológico e de recursos minerais do Estado de Mato Grosso.il Mapas Esc.: 1:1.000.000*. Cuiabá, CPRM/SICME-MT, 235p.

Luz J.S., Oliveira A.M., Souza J.O., Motta J.F.M., Tanno L.C., Carmo L.S.; Souza N.B. 1980. *Projeto Coxipó. Relatório Final*. Goiânia, DNPM/CPRM. v. l, 136 p.

Manzano J.C., Godoy A.M., Araujo L.M.B. 2008. Contexto Tectônico dos Granitóides Neoproterozóicos da Faixa de Dobramentos Paraguai, MS e MT. *Unesp. Geociências*, **27**(4):493-507.

Nishikawa O., Takeshita T. 1999. Dynamic analysis and two types of kink bands in quartz veins deformed under subgreenschist conditions. *Tectonophysics*. **301**:21-34.

Nogueira V.L & Oliveira C.C. 1978. *Projeto Bonito Aquidauana. Relatório Final*. Goiânia, DNPM/CPRM, v.1, 121 p.

Paes de Barros A.J., Costa J.J.G., Resenda W.M. 1998. Tipologia das Mineralizações Auríferas da Fazenda Salinas, Poconé, MT. *In*: Congresso Brasileiro de Geologia, 40, Belo Horizonte, *Bol. de Resumos*, p.235.

Passchier C.W., Trouw R.A.J. (2ed). 2005. *Microtectonics*. Berlin, Springer, 353 p.

Pires F.R.M., Gonçalves F.T.T., Ribeiro L.A.S., Siqueira A.J.B. 1986. Controle das mineralizações auríferas do Grupo Cuiabá, Mato Grosso. *In*: 34 Congresso Brasileiro de Geologia, Goiânia, *Anais*, SBG, v. 5, p. 2383-2395.

Pluijm B.A.V.D., Marshak S. (2 ed). 2003. *Earth Structure: An Introduction to Structural Geology and Tectonics*. New York, W.W. Norton & Company, 656 p.

Seer H.J. 1985. *Geologia, Deformação e Mineralização de Cobre do Complexo Vulcano Sedimentar de Bom Jardim de Goiás*. Dissertação de Mestrado, UNB, Brasília, 181 p.

Seer H.J. & Nilson A. A. 1985. Contribuição à geologia das unidades Pré- Cambrianas da região de Bom Jardim de Goiás. *In*: II Simpósio de Geologia de Centro-Oeste,*Atas*... Goiânia, SBG, p. 267-281.

Silva C.H. 1999.*Caracterização Estrutural de Mineralizações Auríferas do Grupo Cuiabá, Baixada Cuiabana (MT)*. Dissertação de Mestrado, UNESP, Rio Claro, 134 p.

Silva C.H., Simões L.S.A., Ruiz A.S. 2002. Caracterização estrutural dos veios auríferos da região de Cuiabá, MT. *Revista Brasileira de Geociências*, **32**(04):407-418.

Souza N.B. 1981. O Grupo Cuiabá na área do Projeto Coxipó. Estratigrafia e potencialidade econômica. *In*: I Simpósio de Geologia de Centro-Oeste, Goiânia, *Atas*..., SBG, p. 226-239.

Stesky R.M.,Brace W.F.,Riley D.K., Robin P.Y.F. 1974. Friction in faulted rock at high temperature and pressure.*Tectonophysics*, **23**:177-203.

Stesky R.M. 1978. Mechanisms of high temperature frictional sliding in Westerly granite. *Canadian Journal of Earth Sciences*, **15**:361-375.

Stipp M., Stünitz H., Heilbronner R., Schimid S.M. 2002. The Eastern Tonale fault zona: a "natural laboratory" for crystal plastic deformation of quartz over a temperature range from 205 to 700°C. *Journal of Structural Geology*, **24**:1861-1884.

Tokashiki C.C. & Saes G.S. 2008. Revisão estratigráfica e faciologia do Grupo Cuiabá no alinhamento Cangas-Poconé, baixada Cuiabana, Mato Grosso. *Revista Brasileira de Geociências*, **38**(4):661-675.

Van Daalen M., Heilbronner R., Kunze K. 1999. Orientation analysis of localized shear deformation in quartz fibres at the brittle-ductile transition. *Tectonophysics*, **303**:83-107

Vernon R.H. (3 ed). 2004. A *Pratical Guide to Rock Microstructure*. Cambridge, Cambridge, 594 p.

Arquivo digital disponível on-line no site www.sbgeo.org.br